

STANFORD UNIV CA DEPT OF MATHEMATICS
NONLINEAR TWO-DIMENSIONAL SAIL THEORY. (U)
MAR 81 J VANDEN-BROECK

F/G 20/4

UNCLASSIFIED

ARO-16415.172-MA

DAAG29-80-C-0041
MA NL

$$\frac{1}{2} \left(\frac{1}{2} + \frac{1}{2} \right) = \frac{1}{2}$$

END
DATE
FILMED
5 82
DTIC

2

Form 104-104
SECURITY CLASSIFICATION OF THIS PAGE (When Data Entered)

REPORT DOCUMENTATION PAGE		READ INSTRUCTIONS BEFORE COMPLETING FORM
1. REPORT NUMBER 16415.172-MA	2. GOVT ACCESSION NO. N/A	3. RECIPIENT'S CATALOG NUMBER N/A
4. TITLE (and Subtitle) Nonlinear Two-Dimensional Sail Theory		5. TYPE OF REPORT & PERIOD COVERED Reprint
		6. PERFORMING ORG REPORT NUMBER N/A
AUTHOR(s) Jean-Marc Vanden-Broeck		8. CONTRACT OR GRANT NUMBER(s) DAAG29 80 C 0041
PERFORMING ORGANIZATION NAME AND ADDRESS Stanford University Stanford, CA 94305		10. PROGRAM ELEMENT, PROJECT, TASK AREA & WORK UNIT NUMBERS N/A
CONTROLLING OFFICE NAME AND ADDRESS U. S. Army Research Office P. O. Box 12211 Research Triangle Park, NC 27709		12. REPORT DATE Mar 82
MONITORING AGENCY NAME & ADDRESS (if different from Controlling Office)		13. NUMBER OF PAGES 4
		15. SECURITY CLASS. (of this report) Unclassified
		15a. DECLASSIFICATION/DOWNGRADING SCHEDULE
DISTRIBUTION STATEMENT (of this Report) Submitted for announcement only.		
17. DISTRIBUTION STATEMENT (of the abstract entered in Block 20, if different from Report) B		
18. SUPPLEMENTARY NOTES		
19. KEY WORDS (Continue on reverse side if necessary and identify by block number)		
20. ABSTRACT (Continue on reverse side if necessary and identify by block number)		

DTIC
ELECTE
MAY 11 1982
B

ADA 114120

DTIC FILE COPY

Nonlinear two-dimensional sail theory

Jean-Marc Vanden-Broeck^{a)}

Department of Mathematics, Stanford University, Stanford, California 94305
(Received 23 March 1981; accepted 5 January 1982)

Steady two-dimensional flow past a sail is considered. The sail is assumed to be supported by two masts. The flow and the shape of the sail are determined as functions of the direction α of the flow at infinity and the Weber number λ . The full nonlinear problem is formulated as an integrodifferential equation for the shape of the sail. This equation is discretized and solved numerically by Newton's method. Sail profiles, the slack in the sail, and the lift coefficient are presented for various values of α and λ .

I. INTRODUCTION

We consider the deformation of a two-dimensional sail due to the steady potential flow of an incompressible inviscid fluid around it (see Fig. 1). The sail is supported by two masts and is characterized by its constant tension σ and by the distance c between the two masts. The fluid has density ρ and velocity U at infinity. As we shall see, the shape of the sail is determined by the direction α of the flow at infinity and by the Weber number

$$\lambda = 2\rho c U^2 / \sigma. \quad (1)$$

This problem was first considered by Thwaites¹ and Nielsen.² These authors obtained approximate solutions for α small by using thin aerofoil theory. Their work was further generalized by Tuck and Haselgrove³ and Dugan.⁴ More recently, Vanden-Broeck and Keller⁵ obtained an asymptotic solution for λ small for arbitrary values of α .

In the present paper we solve the fully nonlinear problem numerically. In Sec. II we formulate the problem as an integrodifferential equation for the unknown shape of the sail. In Sec. III we present a method to solve this equation numerically. The method involves discretization, which converts the equation into a set of nonlinear algebraic equations. Then it employed Newton's method to solve these equations. The results obtained are discussed in Sec. IV.

Many different families of solutions exist. Tuck and Haselgrove's⁶ stability analysis shows that only one family of solutions is stable for α small. Therefore, we present only numerical results for this family. It is found that for each value of α there is a maximum value of the Weber number λ above which this family fails to exist.

II. FORMULATION

Let us consider the steady two-dimensional flow of an inviscid incompressible fluid past an inextensible and flexible sail. The flow configuration, the sail, and the coordinates are sketched in Fig. 1.

The leading edge or luff of the sail is attached to a mast at $x=0, y=0$ and the trailing edge or leach is attached to another mast at $x=c, y=0$. At infinity we require that the flow have speed U and direction α .

We introduce dimensionless variables by taking c as the unit length and U as the unit velocity. Let the shape of the sail be described in dimensionless variables by $y=F(x), 0 \leq x \leq 1$. The conditions of attachment to the masts imply

$$F(0)=F(1)=0. \quad (2)$$

The difference between the pressures on the two sides of the sail is balanced by $\kappa(x)\sigma$, where κ is the curvature of the sail and σ is the constant tension in it. By using Bernoulli's equation we obtain, in dimensionless variables

$$\kappa(x) = (\lambda/4)[q^+(x)^2 - q^-(x)^2]. \quad (3)$$

Here, $q^+(x)$ and $q^-(x)$ are the flow velocities above and below the sail, respectively. The parameter λ is the Weber number defined by (1).

It is convenient to introduce the complex perturbation velocity

$$a - ib = u - \cos \alpha - i(v - \sin \alpha). \quad (4)$$

Here, u and v denote, respectively, the chordwise and normal components of the velocity. The function $a - ib$ is an analytic function of $z = x + iy$ which vanishes at infinity. Therefore, we can write, by using the Plemelj formula

$$a^+(x) + a^-(x) - i[b^+(x) + b^-(x)] = \frac{i}{\pi} \int_0^1 \frac{[a^+(x_1) - a^-(x_1)] - i[b^+(x_1) - b^-(x_1)]}{(x_1 - x) + i[F(x_1) - F(x)]} dx_1. \quad (5)$$

The integral in (5) is of the Cauchy principal value form.

The velocity must be tangent to the sail on both sides. Thus, we have

^{a)} Present address: Department of Mathematics and the Mathematics Research Center, University of Wisconsin, Madison, Wisconsin 53706.

$$v^+(x) = u^+(x)F'(x), \quad 0 \leq x \leq 1. \quad (6)$$

Using the definition (4), we can rewrite (6) in the more convenient form

$$b^+(x) - b^-(x) = [a^+(x) - a^-(x)]F'(x), \quad (7)$$

$$b^+(x) + b^-(x) = -2 \sin \alpha + [a^+(x) + a^-(x)]F'(x) + 2 \cos \alpha F''(x). \quad (8)$$

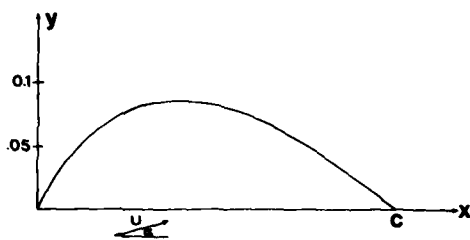


FIG. 1. Computed profile of a sail with $\alpha = \pi/6$, $\lambda = 0.82$, and $\beta = 3.0$. The unit length in y is c .

By substituting (7) into (5) and taking real and imaginary parts we obtain

$$\begin{aligned} b^*(x) + b^-(x) &= \frac{1}{\pi} \int_0^1 \frac{[a^*(x_1) - a^-(x_1)][1 + F'(x_1)^2](x_1 - x)}{(x_1 - x)^2 + [F(x_1) - F(x)]^2} dx_1, \quad (9) \\ a^*(x) + a^-(x) &= -\frac{1}{\pi} \int_0^1 \frac{[a^*(x_1) - a^-(x_1)][1 + F'(x_1)^2][F(x_1) - F(x)]}{(x_1 - x)^2 + [F(x_1) - F(x)]^2} dx_1. \quad (10) \end{aligned}$$

$$\frac{1}{\pi} \int_0^1 \frac{[1 + F'(x_1)^2][a^*(x_1) - a^-(x_1)](x_1 - x) + F'(x)[F(x_1) - F(x)]}{(x_1 - x)^2 + [F(x_1) - F(x)]^2} dx_1 = -2 \sin \alpha + 2 \cos \alpha F'(x), \quad (13)$$

$$\frac{F''(x)}{[1 + F'(x)^2]^{3/2}} + \frac{\lambda}{4} [a^*(x) - a^-(x)][1 + F'(x)^2] \left(2 \cos \alpha - \frac{1}{\pi} \int_0^1 \frac{[a^*(x_1) - a^-(x_1)][1 + F'(x_1)^2][F(x_1) - F(x)]}{(x_1 - x)^2 + [F(x_1) - F(x)]^2} dx_1 \right) = 0. \quad (14)$$

This system is solved numerically in the next section.

From the solution we can then compute the slack l in the sail by the formula

$$l = \int_0^1 \{1 + [F'(x)]^2\}^{1/2} dx - 1. \quad (15)$$

Following Thwaites¹ we define the parameter β by the relation

$$\beta = \sin 2\alpha / 2l^{1/2}. \quad (16)$$

The lift coefficient is obtained from the solution by substituting (7) into the formula (15) given by Vanden-Broeck and Keller.⁵ Thus, we obtain

$$C_L = \left| 2 \int_0^1 [a^-(x) - a^*(x)][1 + F'(x)^2] dx \right|. \quad (17)$$

III. NUMERICAL ANALYSIS

In order to solve the system of equations defined by (2), (12), (13), and (14) we introduce the mesh points

$$x_I = (I-1)/(N-1), \quad I = 1, \dots, N, \quad (18)$$

and the corresponding unknowns

$$F_I = F(x_I), \quad I = 1, \dots, N, \quad (19)$$

$$A_I^- = a^-(x_I) - a^+(x_I), \quad I = 2, \dots, N. \quad (20)$$

Relations (2) and (12) imply $F_1 = F_N = 0$ and $A_N^- = 0$, so that there are only $2N-4$ unknowns F_I and A_I^- .

We shall satisfy Eqs. (13) and (14) at the $N-3$ inter-

We now rewrite (3) in the form

$$\begin{aligned} \frac{F''(x)}{[1 + F'(x)^2]^{3/2}} + \frac{\lambda}{4} [a^*(x) - a^-(x)][1 + F'(x)^2] \{ 2 \cos \alpha \\ + a^*(x) + a^-(x) \} = 0. \end{aligned} \quad (11)$$

Finally, we impose the Kutta condition at $x=1$ by requiring

$$a^*(1) = a^-(1). \quad (12)$$

The condition (12) is clearly not satisfactory when

$$F'(x) \sim (1-x)^\nu \quad \text{with } \nu \leq -\frac{1}{2} \text{ as } x \rightarrow 1.$$

However, such exceptional cases did not occur in the numerical solution. We shall consider only values of α between 0 and $\pi/2$ so that the Kutta condition is imposed at the trailing edge.

For given values of λ and α relations (8)–(12) define a nonlinear system of integrodifferential equations for the unknowns $F(x)$, $a^*(x)$, $a^-(x)$, $b^*(x)$, and $b^-(x)$.

By substituting (7), (9), and (10) into (8) and (11) we obtain the following reduced system of equations for the two unknowns $a^*(x) - a^-(x)$ and $F(x)$:

mediate mesh points

$$x_{I+1/2} = (x_I + x_{I+1})/2, \quad I = 2, \dots, N-2. \quad (21)$$

First, we compute $F'(x_I)$, $F'(x_{I+1/2})$, $F''(x_{I+1/2})$, $F(x_{I+1/2})$, and $a^-(x_{I+1/2}) - a^+(x_{I+1/2})$ in terms of F_I and A_I^- by four point formulas.

Next, we evaluate the integrals in (13) and (14) by using the trapezoidal rule with the mesh points x_I . The mesh points x_I are locally symmetric about $x_{I+1/2}$ and the quadrature formula is also symmetric. Therefore, the contribution from the neighborhood of the singularity cancels out, permitting us to evaluate the Cauchy principal value as if it were an ordinary integral.

In doing so it is important to notice that the integrands in (13) and (14) behave like $x^{-1/2}$ as $x \rightarrow 0$. We handle these singularities by subtracting the singular part before integrating numerically. We then integrate the singular part analytically.

By discretizing (13) and (14) we obtain $2N-6$ nonlinear algebraic equations for the $2N-4$ unknowns F_I and A_I^- . An extra equation is obtained by imposing the Kutta condition at $x=1$ via the relation

$$\lim_{x \rightarrow 1} (1-x)^{1/2} [a^*(x) - a^-(x)] = 0. \quad (22)$$

A three-point Lagrange extrapolation formula is used to evaluate the limit in terms of A_I^- . The last equation is obtained by imposing (2) by means of a three-point

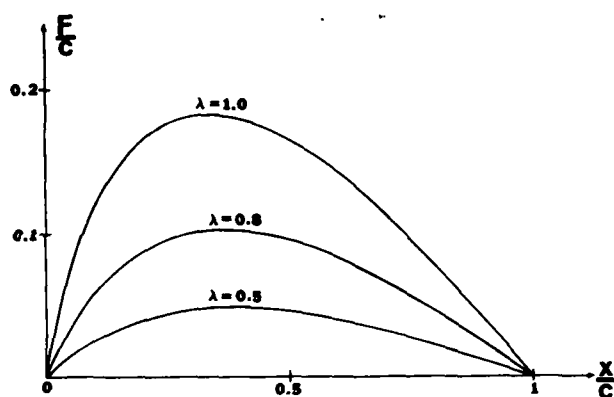


FIG. 2. Computed profiles of a sail with $\alpha = \pi/4$ of $\lambda = 0.5$, 0.8 , and 1.0 . The corresponding values of β are, respectively: 6 , 2.8 , and 1.6 . The unit length in which both x and y are measured is c .

Lagrange formula.

For given values of λ and α this system of equations is solved by Newton's method. The values of β and C_L can then be computed by quadrature from (16) and (17).

IV. DISCUSSION OF THE RESULTS

We have used the method described in Sec. III to compute solutions for various values of λ and α . Many different families of solutions exist. They have been studied for α small by Thwaites.¹ These families can be computed for arbitrary α and λ in the following way. For a given value of λ we compute the solution for a small value of α by using the uniform stream (i.e., the solution corresponding to $\alpha = 0$) as the initial guess. Provided that λ is not close to any of the critical values described by Thwaites,¹ the numerical scheme converges rapidly to his solution for the given value of λ . Once a given solution has been obtained, however, a type of "boot-strap" technique is employed, that is, a converged solution for one value of λ is used as the initial guess for a solution with λ altered by a few percent. Similarly, for fixed λ , the angle α could be varied

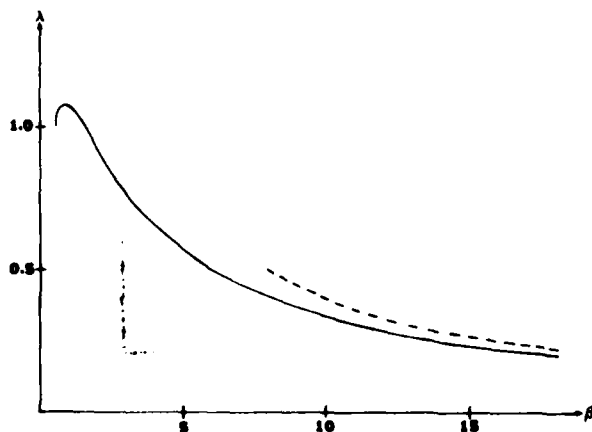


FIG. 3. Values of the Weber number λ as a function of β for $\alpha = \pi/4$. The dashed curve corresponds to Vanden-Broeck and Keller's asymptotic formula.

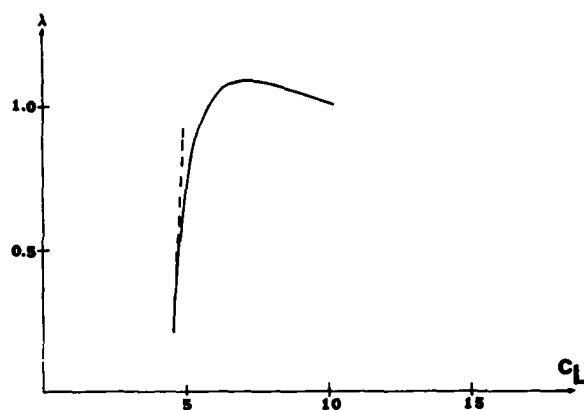


FIG. 4. Values of the lift coefficient C_L as a function of β for $\alpha = \pi/4$. The dashed curve corresponds to Vanden-Broeck and Keller's asymptotic formula.

using a neighboring solution as a starting guess.

Among all these possible solutions, only one is "reasonable" in the sense that it has a simple unimodal shape cambered to lee of the wind. Tuck and Haselgrove's⁶ stability analysis shows that this family of solutions is the only stable one for α small. Therefore, we extend only this family to the nonlinear case.

Typical profiles are shown in Figs. 1 and 2. The values of β and C_L for $\alpha = \pi/4$ are shown as functions of λ in Figs. 3 and 4. The broken lines correspond to the asymptotic formulas (14) and (20) given by Vanden-Broeck and Keller.⁵ The asymptotic formula for β agrees with the numerical results within fifteen percent for $\lambda < 0.3$.

In Fig. 5 we present the values of λ vs β for $\alpha = \pi/100$ and $\alpha = \pi/10$. The broken line corresponds to Thwaites' solution. It shows that his solution is a good approximation for α small, but it is not uniform as β tends to zero. The discrepancy between his solution and the exact numerical solution increases rapidly as β gets close to zero. In the particular case $\beta = 1$, the values of C_L were computed for various values of α . The numerical values of C_L were found to agree with Thwaites' solution within 5% for $\alpha \leq \pi/18$, 20% for $\alpha \leq \pi/6$, and 30% for $\alpha \leq \pi/4$.

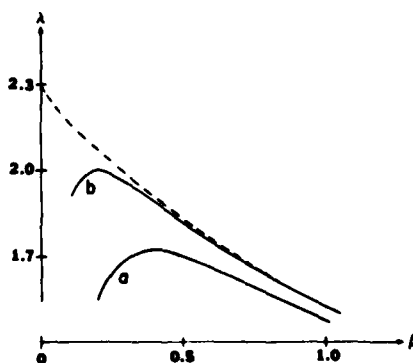


FIG. 5. Values of the Weber Number λ as a function of β for $\alpha = \pi/100$ (curve a) and $\alpha = \pi/10$ (curve b). The dashed curve corresponds to Thwaites' calculations.

Figures 3 and 5 and similar results obtained for different values of α indicate that for each value of α there exists a maximum value $\lambda_0(\alpha)$ of the Weber number above which there is no solution of the kind considered here. For a given value of α there are two solutions for each value of the Weber number in an interval below the maximum value. This nonuniqueness is likely to be of mathematical interest only. The reason for this is that the branch on the left of the maximum is probably unstable. After all, it corresponds to an increase of the tension arising from an increase in the slack. This suggests that the physically realizable solutions corresponds to $\lambda \geq \lambda_0(\alpha)$.

As α increases, the slope of the profile increases at the leading edge. This was found to limit the accuracy of the numerical scheme. Accurate solutions for $\alpha \geq \pi/3$ and $\lambda \sim \lambda_0(\alpha)$ could not be computed with $N \leq 35$.

Finally, it is worthwhile mentioning that the present model is not physical for α large since separation is

then likely to occur. A more realistic model for α large was proposed by Dugan.⁴

ACKNOWLEDGMENTS

This work was supported by the Office of Naval Research, the Air Force Office of Scientific Research, the National Science Foundation, and the Army Research Office at Stanford University, and by the United States Army under Contract No. DAAG 29-80-C-0041, and the National Science Foundation under Grant No. MCS-7927062, Mod. 1, at the Mathematics Research Center.

¹B. Thwaites, *Proc. R. Soc. London Ser. A* **261**, 402 (1961).

²J. N. Nielsen, *J. Appl. Mech.* **E 80**, 435 (1963).

³E. O. Tuck and M. Haselgrove, *J. Ship Res.* **16**, 148 (1972).

⁴J. P. Dugan, *J. Fluid Mech.* **42**, 433 (1970).

⁵J.-M. Vanden-Broeck and J. B. Keller, *Phys. Fluids* **24**, 552 (1981).

⁶M. K. Haselgrove and E. O. Tuck, in *New England Sailing Yacht Symposium* (Society of Naval Architects and Marine Engineers, New York, 1976).



Accession For	
DTIC GRAFI	<input checked="" type="checkbox"/>
DTIC TAB	<input type="checkbox"/>
Unannounced	<input type="checkbox"/>
Justification	
By	
Distribution	
Availability Codes	
Avail and/or	
Dist	
A	21